



**Recent Advancement in Chiral Spintronics from Molecular Level to Device Application.
A prospect based on the interplay between physical and chemical properties of chiral system**

Journal:	<i>Journal of Materials Chemistry C</i>
Manuscript ID	TC-PER-08-2024-003453.R1
Article Type:	Perspective
Date Submitted by the Author:	19-Nov-2024
Complete List of Authors:	Mishra, Suryakant; Los Alamos National Laboratory, Center for Integrated Nanotechnologies, Materials Physics and Applications Division Jones, Andrew; Los Alamos National Laboratory, Center for Integrated Nanotechnologies, Materials Physics and Applications Division Fontanesi, Claudio; University of Modena and Reggio Emilia, Engineering

Recent Advancements in Chiral Spintronics from Molecular Level to Device Applications.

A prospect based on the interplay between physical and chemical properties of chiral systems.

Suryakant Mishra^{1*}, Andrew C. Jones^{1*}, Claudio Fontanesi^{2*}

¹Center for Integrated Nanotechnologies Los Alamos National Laboratory Los Alamos, NM 87545, USA

²Department of Engineering 'Enzo Ferrari' DIF University of Modena and Reggio Emilia Via Vivarelli 10, Modena 41125, Italy

*mishras@lanl.gov, acj@lanl.gov, claudio.fontanesi@unimore.it

Abstract

This review relates recent advancements in chiral-based spin-electronic devices obtained using suitable combinations of organic, inorganic and hybrid materials. Specifically, the focus is on how chirality can be suitably used to control spin in practical applications, with reference to spintronic sensors and consumer devices. Interestingly, the physical mechanism by which that control can be implemented is the chiral-induced spin selectivity (CISS) effect, which connects the structural chirality of a material with its electronic spin-selective transport properties. The CISS effect is based on the observation that the charge transmission in chiral systems is spin selective, this experimental evidence points to the existence of a relation between the electron spin and the structural handedness of the matter. This unique structure/transport relationship can be exploited in designing a wide number of spintronics devices, from memory to transistors, logic gates and molecular q-bits.

Keywords: CISS, Spintronics, Optoelectronics, Chiral induction, Spin-dependent electrochemistry

1. Chirality and Chiral Induced spin-selectivity (CISS) effect

Chirality is an exceptionally transversal and interdisciplinary field of science, profoundly connected to biology, chemistry, physics and mathematics as well, as shown in Figure 1. It is observed in nature from most fundamental molecule of life such as DNA and protein to the macroscopic level such as nautilus, shells, snail, flowers, or imprinting of clockwise and counter-clockwise rotating permanent magnetizations in soil and ground material due to corresponding positive and negative polarities of lightning current.^{1,2} Chirality as a concept is often conveyed in terms of the left and right handed specular images, which is by far an over-simplified picture i) Barron suggested the classification of “true” and “false” chirality, where true chirality refers to time-invariant enantiomorphism and false chirality to time-noninvariant enantiomorphism^{3,4} ii) fundamental physical quantities as the angular momentum, the magnetic field associated with a current (Biot-Savart law) and the spin are tightly related to the concept of handedness, just to mention a few.² Topics deeply related with the concept of handedness, and apparently unrelated to “chirality/handedness”, are 1) magnetism, where polar and axial vectors play a central role² 2) spin and all of the related implications and applications spintronics (spin-valve based logic gates).⁵⁻⁷

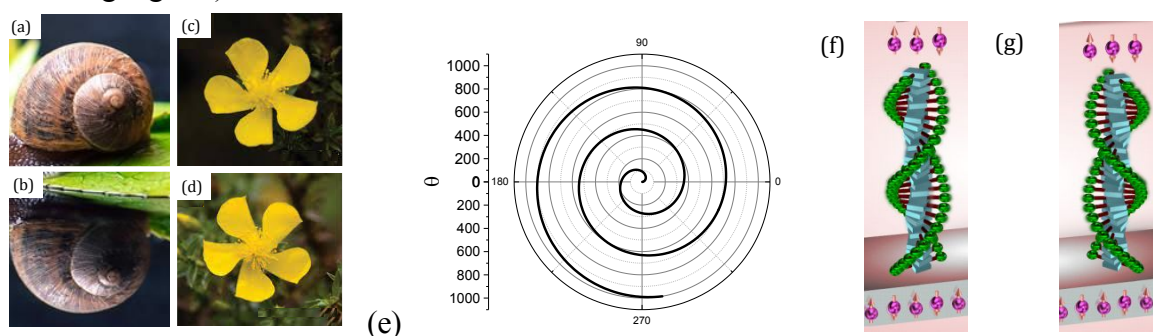


Figure 1: Chirality in nature (a-d), in 2d geometry: Archimedean spiral $r(\theta) = \theta$ calculated in the $0 < \theta < 1000$ range (e), schematic presentation of Chiral induced spin selective effect when chiral molecule is in contact with ferromagnetic substrate(f,g).^{8,9}

Moreover, just thinking of how nature developed life on planet Earth gives a clear idea of the importance of chirality: with few exceptions, it is well-known the great majority of amino acids, proteins, and bio-related molecular architectures are chiral and present a single handedness in nature. i.e. proteins are typically right-handed, this is known as the “homochirality problem”, a yet to be solved fundamental conundrum.¹⁰ Applications concerning chirality span from 1) sensors¹¹⁻¹³ able to detect important molecules for human health like insulin and glucose 2) separation (resolution) of racemic mixtures¹⁴⁻¹⁷ 3) drug synthesis in pharmaceutical industry 4) chemical reactivity¹⁸⁻²⁰ 5) chiral induction^{21,22} 6) light-driven molecular motors.²³ Chiral recognition and enantioselectivity are commonly assumed to arise from a simple geometrical effect (a vision especially well rooted within chemists and biologists), typically described by “lock and key” and “Three-Point Interaction” qualitative models.²⁴

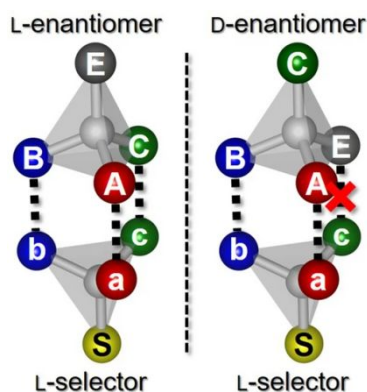


Figure 2: Schematic representation of the three-point chiral-recognition model, depending on the enantiomer handedness, L or D, with fixed orientation of the chiral “selector”. The sites ‘A’, ‘B’, and ‘C’ experience different interactions with the ‘a’, ‘b’, and ‘c’ centres. Reproduced from reference 25 with permission from Nature Publishing Group, copyright 2020.

Thus, chiral recognition, and enantioselectivity as well, are still sitting on the Three-Point Interaction cartoon as represented in Figure 2, although it was proven to be not effective in a number of cases.²⁵ Recently, spin-based exchange interactions have been proposed to rule chemical reactivity in the field of chiral-induction, i.e. the ability of a chiral compound to induce chirality in an achiral system.²⁶

Moreover, the physics underlying the emerging of specific interactions between chiral systems and spin polarized electrons is currently an open question, together with electro magneto-chiral dichroism^{7,19,27} and the Chiral Induced Spin-Selectivity (CISS) effect.^{19,28–31}

Beyond the high purely scientific interest, CISS effect recent results obtained in inorganic systems such as chiral crystals,³² perovskite^{33,34} and MOF with hybrid organic/inorganic composition,³⁵ pave the way towards the development of stable spintronic devices to be developed within the CISS framework, by using suitably designed chiral materials. Indeed, in some of the explored systems spin polarization values not far from 100% have been observed till this date.^{6,36}

1.1 The CISS effect

In a nutshell the CISS effect is the recognition that a flow of electrons transmitted through a chiral system emerges as spin-polarized, as it is schematically depicted in **Figure 3**.

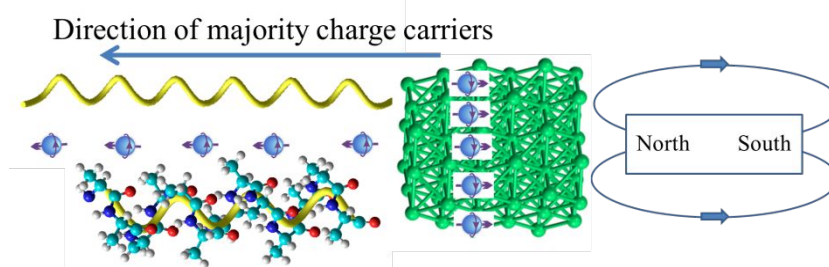


Figure 3: Schematic representation of the CISS effect. A ferromagnetic material, under the application of a magnetic field, is exploited as a spin injector. An adsorbed layer of chiral enantiopure polypeptide acts as a spin-filter.

1.2 Theoretical models for the CISS effect

The theoretical understanding of the physics underlying CISS remains a subject yet open to discussion. Indeed, recent theoretical papers comparing charge transmission in achiral vs

chiral simple organic systems, show that a fundamental role is played by spin-orbit coupling (SOC), **Figure 4**,³⁷ in the charge transmission process,³⁸ and that charge transmission is much more efficient in the case of chiral systems.³⁹

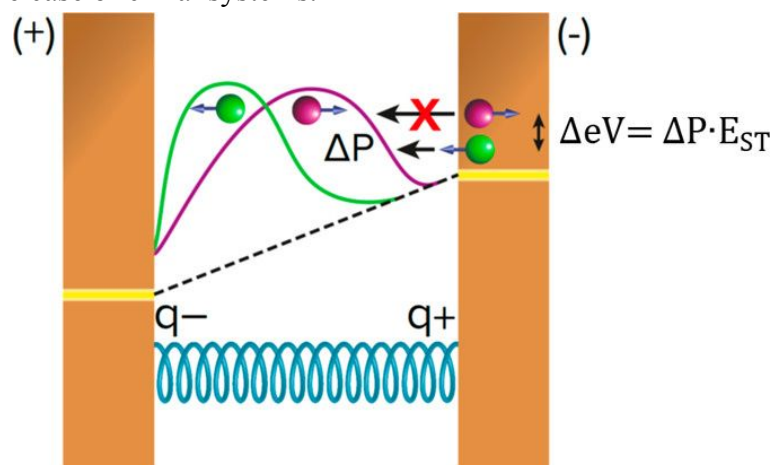


Figure 4: Schematic representation of how SOC, in a system with handedness, could induce spin-filtering, i.e. CISS effect. The small spin polarization, ΔP , arises from the SOC, and causes a spin blockade because of the Pauli principle. Which is proportional to the singlet–triplet energy gap, E_{ST} , in the molecule. The purple and green curves represent the charge distribution occurring upon applying the electric field across the system featuring handedness, here presented schematically as a coil. The yellow and dotted lines represent the electrodes Fermi energy and the electric field across the system. Reproduced from reference 37 with permission from American Chemical Society, copyright 2020.

Then some recent articles address the role of electronic properties, “helical” molecular orbitals, in promoting spin polarization even in the case of tunnelling-base charge transport.^{38,40,41} Continuum effective model for electrons in the helical molecules causes robust coherency in the electron tunnelling⁴² and Onsager reciprocity explains the coupling energy between the contact and chiral molecular are the defining parameters which cause spin polarization.^{43,44} A rather different view underlies the approach of Jonas Fransson,⁴⁵ where the spin-selective effect was proposed to be due to selective scattering with chiral phonons, a particularly interesting approach since it is able to correlate spin-polarization as a function of temperature.³²

Anyhow, the theoretical explanation of the CISS effect is still an open ground, apparently also featuring a rather high parcellation in addressing different forms of effects related to spin-filtering: theory of CISS in transmission, in transport, in chemical reactions.⁴⁶ Indeed, a crucial aspect is how to properly measure/quantify handedness-induced-effects on the electron spin, involving the measurement of suitable quantities, like optical rotation or Hall-potential, or quantification of products following a chemical reaction in classical wet-chemistry synthesis, enantiomeric excess (ee%). Basically, every possible application relies on typical experimental tools to probe the effect of chiral-induced spin-selectivity. This perspective deals with the CISS effect, and thus the main focus regards the electron spin/handedness interactions and the different possible ways to detect and quantify the relevant experimental manifestation. Of course a major role here is played by the detection of spin-polarization (SP%), even though in the field of CISS, due to the various strategies to get at SP% this is a subject which needs to be rationalized.^{47–49}

2. Recent Demonstration of Spin Polarization in Various Molecular System

Spintronics is emerging as a crucial applicative field relevant to recent developments in electronics, related to the implementation of quantum computing technologies, where organic based semiconductors appear of particular interest for practical applications⁵⁰, of course the possibility to couple the flexibility of tailoring complex molecular architectures with CISS paves the way to a number of possible experimental approaches to the problem of how get control on spin polarized currents.

2.1 Hall detection in solid state device

In the case of CISS related measurements the typical Hall-device working principle is overturned: in fact, in a typical Hall-device the so-called Hall potential difference stems from the application of an external magnetic field orthogonal to a current flowing in a conductor.⁵¹ This concept is reversed in the case of a Hall-device designed to detect spin-filtering due to the CISS effect. In this latter case, the Hall device is patterned on a AlGa_N/Ga_N high electron mobility transistors (HEMT) heterostructure, featuring a 2-dimensional electron gas (2DEG) structure 20 nm below the device surface, the channel. Enantiopure chiral molecules are adsorbed on top of the Ga_N surface. Measurements can be operated in two modes, one is polarization induced spin measurement and the other one is spin-polarization obtained via charge transfer, in both cases spin-polarization is obtained applying a potential difference to the Ga_N surface, via an electrochemical cell placed directly on top of the Hall device. Indeed, measurements exploiting such a complicated experimental setup, showed to be capable to measure spin-polarization due to the CISS effect in both solid-state configurations⁵² and wet-chemistry.^{26,53} Here, **Figure 5** summarizes the results in terms of Hall potential, obtained at varying systematically the thickness of the chiral interface: oligopeptides and DNA base pairs adsorbed on the Ga_N surface of the AlGa_N/Ga_N HEMT, which is the channel of the Hall device.⁵⁴ The integrated electrochemical cell/Hall-effect based device allows to measure a Hall potential due to spin accumulation in the AlGa_N/Ga_N channel, due to the CISS effect, i.e. spin filtering, inducing spin-accumulation the Hall-device channel, creation of a magnetic field due to spin accumulation.^{26,52,53} The Hall device, featuring the chiral interface, was embedded inside a buffer solution, and a gate insulated from the solution, was located on top of the device, as schematized **Figure 5(a)**. By applying electric potential between the gate and the Hall device, the adsorbed molecules were polarized (in fact spin-polarized, in the case of an enantiopure chiral interface), as schematized in **Figure 5(b)**. The spin polarization, which accompanied the charge polarization, was monitored by measuring the Hall potential. In short, the electrochemical driven, electric field polarization induces spin-polarization, and eventually a Hall voltage is measured in the device (due to presence of spin-polarization, hence an associated magnetic field).^{26,53}

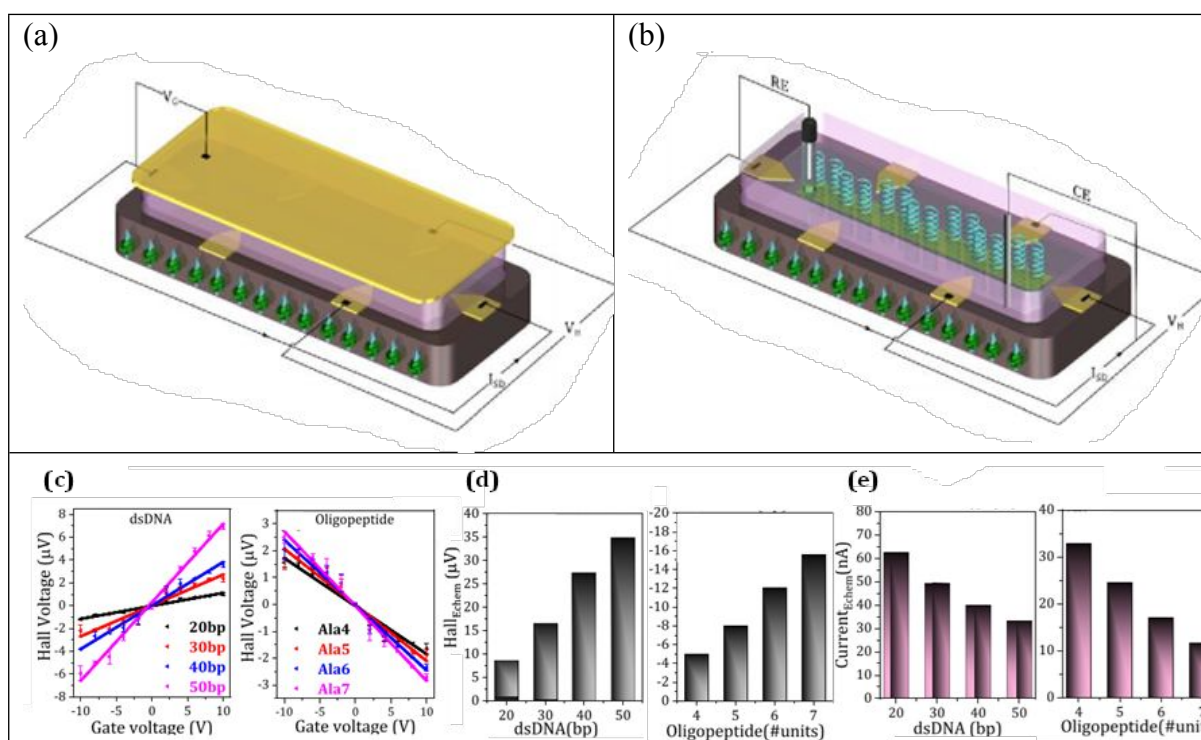


Figure 5: Schematic illustration of the Hall device for both polarization and spin-electrochemistry mode (a & b), Hall voltage recorded during the polarization mode gives the information about the spin polarization in DNA and oligopeptide (c), Hall voltage (d) and corresponding electrochemical current (e) recorded during the electrochemistry measurement on DNA and oligopeptide. Reproduced from reference 54 with permission from American Chemical Society, copyright 2020.

In the case of charge transfer wet-chemistry, a spin dependent electrochemical current is obtained by using a standard three electrodes electrochemical cell, where the Hall-device itself serves as the working electrode. In this case the Hall voltage is the measure of spin selective charge transfer from redox couples in bulk solution or chemisorbed on the Hall-device. **Figure 5(b)** summarizes the results obtained by this type of studies of interphases built exploiting various chiral compounds such as DNA and oligopeptides of varying length. These molecules of different lengths are thiol-terminated and were immobilized on the gold channel of a Hall device chip for spin selective measurements. **Figure 5(c)** sets out the result of Hall voltage measurement as a function of the self-assembled monolayer (SAM) thickness: in units of dsDNA base-pairs and oligopeptide repeating units, i.e. as a function of the length of adsorbed molecules. Remarkably, the Hall potential, for a constant gate voltage, increases as the thickness of the chiral interface increases, in addition the Hall-potential change in sign is consistent with changing the sign of the gate voltage. A linear relationship holds between the thickness of the chiral interface and the Hall potential, as shown in **Figure 5(d)**. Eventually, note that the Hall potential (the degree of spin-polarization to a first approximation) increases and the electrochemical current decreases. A results consistent with previously published experimental results.⁵⁵

2.2 Hall detection using 3D-electrochemical cell

The CISS effect detection relying on electrochemical measurements is a topic growing in interest.^{56,57} Here it is demonstrated how a classical electrochemical setup is integrated with a Hall-device, again exploiting a GaN/AlGaN heterostructure with 2-dimensional electron gas (2DEG) which is acting simultaneously as the working electrode of an electrochemical cell and the channel of Hall-effect device: in an experiment coded as three-dimensional spin-dependent electrochemistry (3D-SDE).²⁶

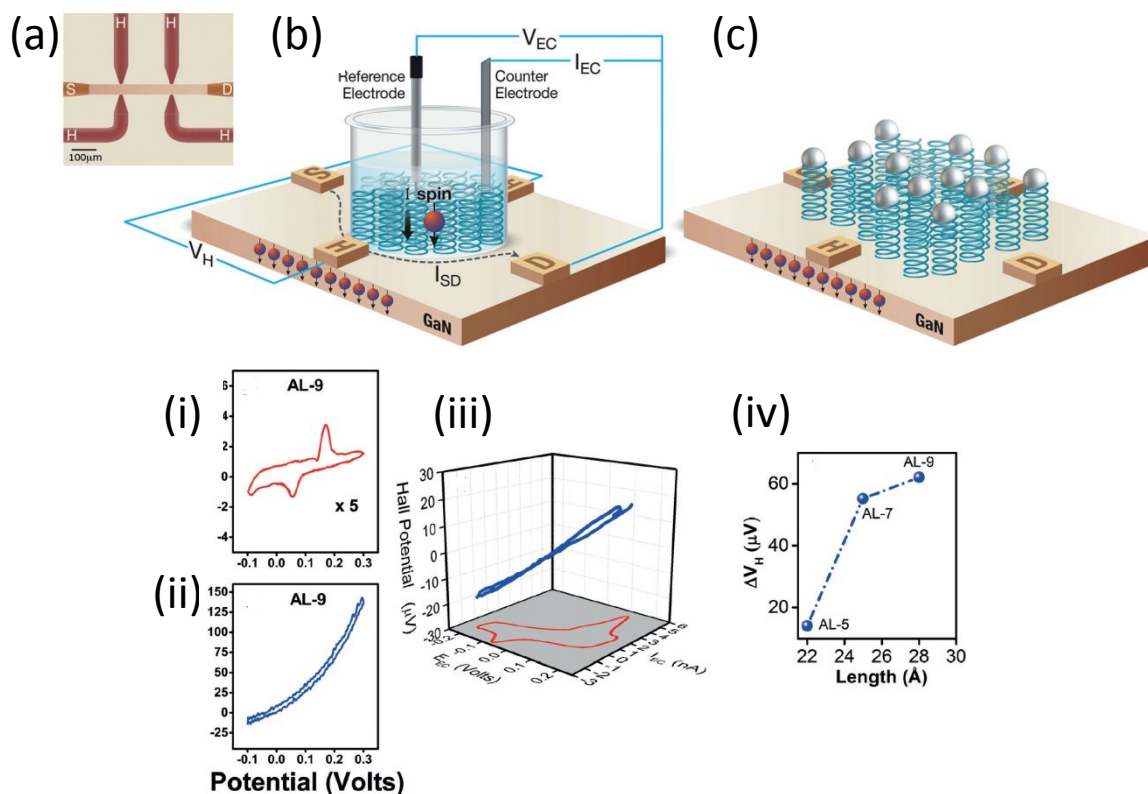


Figure 6: Optical image of the actual hall device(a) along with schematic illustration of the device 3D-spin electrochemical system (b) and sample with silver quantum dots (QDs) (c). (i) and (ii) corresponding measurements of spin current and Hall potential. (iii) 3D graphical representation of the experimental data concerning the applied potential, current and Hall potential. (iv) Hall potential as a function of the chiral adsorbed monolayer thickness. Reproduced from reference [26] with permission from John Wiley and Sons Ltd, copyright 2017.

Eventually, it is obtained a quantitative relationship between V_{Hall} vs Monolayer-thickness, **Figure 6** (iv). Suggesting a tight relationship between the Hall potential (which is due to the spin selectivity), induced by the electrochemical potential which is driving the charge transfer across the Hall-device/solution interface, and the length (thickness) of the chiral interface (adsorbed enantiopure peptides). In addition, the Hall device it proved to be able to discriminate surface handedness chiral recognition in Hall/cyclic-voltammetry curves concerning the case of enantiopure chiral ferrocene (FC) redox probe. The latter present in bulk solution. In this experimental architecture a fundamental role is played by the presence of the 2DEG, as it is

discussed in detail in the relevant paper, the physics underlying the essential presence of a 2DEG is yet to be understood.

2.2 Magneto-conducting AFM:

Recent advancements in experimental aspect of the CISS effect concern molecular architectures spanning from supramolecular structures³⁶ to helicenes⁵⁸ and chiralized (chirality is induced by the presence of an asymmetry inducer, quite often the camphor sulfonic acid is used) polymers⁵⁹, also inorganic systems such as Ni oxide⁶⁰ and perovskites by Vardeny group,^{6,34} cobalt and copper oxide^{61,62} and some 2D materials.⁶³

In a recent paper it has been obtained a rather high spin-polarized charge transmission in chiral-induced poly aniline (cPANI). Aniline was used to create a chiral polymer in the presence of an asymmetric catalyst: enantiopure R- and S-camphor sulfonic acid. In-situ chiral induction during electropolymerization clearly shows the handedness present in both the R-cPANI (R-camphorsulfonic acid chiral induced PANI) and S-cPANI (S-camphorsulfonic acid chiral induced PANI). Theoretical calculation proved that helicity in polymer is induced by coupling of chiral catalyst via exchange interactions. Magnetic field dependent AFM measurement shows around 55% spin polarization, $SP\%$, calculated by using equation $SP = (I_{up} - I_{down}) / (I_{up} + I_{down}) * 100$. Chiralized cPANI turned out to be a very robust and consistent system, featuring a quite stable over time spin selective charge transmission (compared to SAM adsorbed at the electrode/solution interface). **Figure 7a** sets out the schematic of magneto-conductive AFM (mcAFM) measurement. Note that, the current in both the magnetization directions was recorded on several spots on the sample surface, and the final average data are presented in the **Figure 7 (b) & (c)**. Remarkably, note the symmetric behaviour of the current vs potential curves upon flipping the magnet (north Up and Down) placed under the electrode, the flipping of the magnet reverse the majority of the spin carrier in the bottom nickel electrode (substrate), on the whole this gives the information about the spin filtering capability of the chiralized PANI polymer.

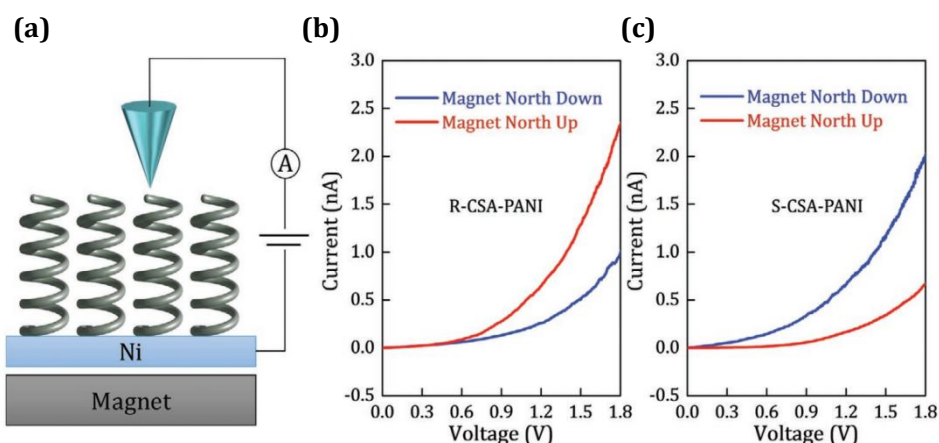


Figure 7: (a) Magnetic conducting probe AFM measurement (mcAFM) in the presence of 0.3 T external neodymium magnet. Averaged current voltage (I-V) scan for (b) R-CSA/PANI and (c) S-CSA/PANI. Reproduced from reference 31 with permission from John Wiley and Sons Ltd, copyright 2020.

2.3 Magnetoresistance Detection

Magnetoresistance (MR) detection is another experimental technique able to characterize the behaviour of a spintronic devices, likewise spin-valves which can be used to probe further the dependence between “molecular structure” and the CISS effect.^{39,64} By means of MR measurements it has been recently demonstrated spin polarization in an inorganic chiralized material, chiral imprinted nickel, prepared using an organic chiral template (enantiopure tartaric acid).⁶⁰ Where chiral-induction was obtained *via* electrochemical co-deposition of nickel in a solution containing enantiopure tartaric acid. **Figure 8** shows the spin valve fabricated using chiral Ni and the relevant device configuration and magnetoresistance results. Asymmetric nature during the magnetic scan was observed which shows spin filtering behaviour coming from chirality of Ni and while switching handedness of the system it gives opposite behaviour in spin filtering. Around 1% MR signal is observed from both the helicity in this spin valve device, which is comparatively lower than the organic counterpart, but this device was more robust upon time and the thickness of the chiral Ni was easily tuneable during the electrochemical deposition. In addition, helicity of nickel was also tuneable by simple switching of the enantiopure catalyst handedness in the electrochemical bath.

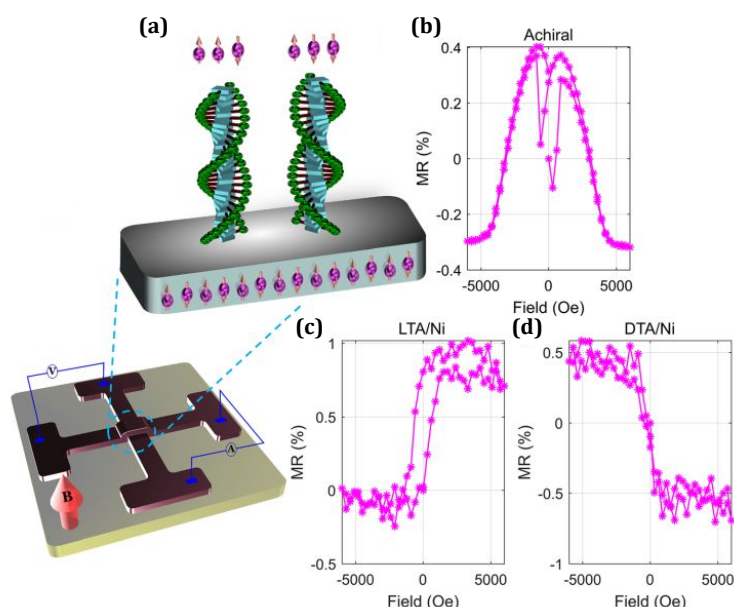


Figure 8: (a) Schematic representation of the magnetoresistance (MR) device, experimental setup: a standard 4-probe configuration is implemented. (b) MR plot with a magnetic field measured on achiral Ni as a cross-check experiment. (c) and (d) on chiral imprinted Ni, L-TA and D-TA, respectively. Reproduced from reference 60 with permission from American Institute of Physics, copyright 2021.

Another example where CISS based spin-polarization is demonstrated exploiting various technique such as mcAFM, Hall measurement and MR measurement to probe the spin polarization in a perfectly mirror symmetric and well-ordered controlled polymer on the surface.⁶⁵ These polymers are thiol (-SH) terminated and able to bind on the gold surface synthesized using a novel polymerization system. The polymers are poly (4-ethynylbenzoyl-l-alanine decyl ester), poly (4-ethynylbenzoyl-d-alanine decyl ester), and poly (4-ethynylbenzoyl-2-methylalanine decyl

ester) (poly-2) named as poly-1L and poly-1D. This was one of a kind of CISS study, where chiral polymer were perfectly oriented on the surface (as it was verified by FTIR and AFM measurements).

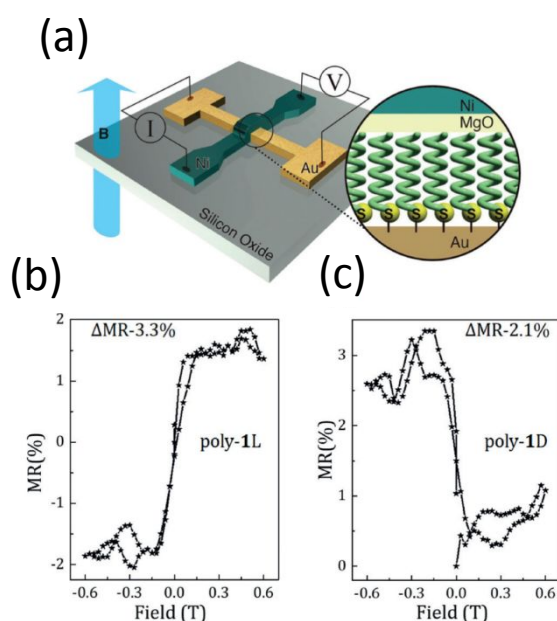


Figure 9: Schematic presentation of spin valve, or MR, a device by incorporating chiral molecular system in a 4-probe geometry (a) MR measurement when poly-1L is used (b) and when opposite chirality (poly-1D) used (c). The opposite z shape of MR curve signifies that the spin filtering property depends on chirality of the device. Reproduced from reference 59 with permission from John Wiley and Sons Ltd, copyright 2020.

Also, one of the interesting features about these polymers is that they are not intrinsically chiral, but chirality is associated with chiral side group which defines the handedness of the polymer. One of the techniques presented in this work, in **Figure 9**, is to measure magnetoresistance and have shown around 3% change in MR value with reverse Z-type pattern observed by switching the chirality, compare results in **Figure 9** (a) & (b).

3. Spintronic Devices within CISS Framework:

3.1 Probing chiral in-plan chiral crystal

Recently, several papers appeared on high impact journals, where handedness is induced in perovskite and crystals of inorganic complexes. These systems are functional to demonstrate the CISS effect, along with various spintronic applications such as in spin-valve devices or related to circularly polarized light emission. In one of such kind of study, authors resolved the crystal structure of mirror symmetry crystals with spatially resolved electrical measurements.⁶⁶ In this work devices based on the spin Hall and inverse spin Hall mechanism to show charge to spin correlation.⁶⁶ One of the interesting results of these measurements is to probe non-local CISS effect, and spatial probing of spin-polarization in the form of charge current. Measured potential difference at three places on the crystal designated as left, right and center electrode while flowing current from the outermost gold electrode is shown in **Figure 10** (b). This is one of the significant studies where opposite effect in polarity of the voltage have been measured, with respect to

changing the handedness of the crystals, with the observation of spin polarization effects on a $10\mu\text{m}$ length scale.

To understand in deep the physical details underlying the observed dependence of spin-polarization on the applied potential difference, i.e. the charge transmission to spin correlation, authors have performed electrical measurements in the presence of the external magnetic field. Both the measurements correlate consistently with the spin effect during charge transfer, which causes opposite polarity in the voltage. Although the causes of spin coherence observed to $10\mu\text{m}$ length scale remain to be understood, if it is not supported by higher spin orbital coupling. Authors also tried to explain this mechanism by spin Hall and inverse spin Hall effect by measuring spin charge current in the central tungsten electrode, in both the crystal by applying constant current in the axis direction.

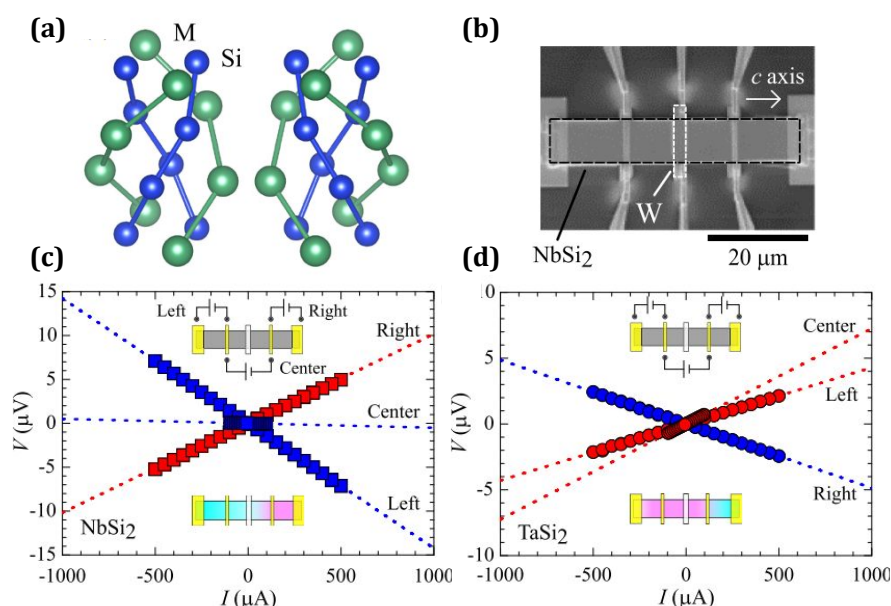


Figure 10: Crystal structures of a disilicide in both mirror symmetric forms (a). Electron microscopic image of the fabricated device on a NbSi_2 crystal, for CISS related measurement (b). Various CISS related measurement were carried out on this geometry while flowing current along the chiral symmetric plan to determine the handedness of system (c) & (d). Reproduced from reference 68 with permission from Nature Publishing Group, copyright 2019.

3.2 Perovskite for chiral emission (spin-LED):

In a recent and elegant example of optical rotation essentially due to the CISS effect, Kim et. al have demonstrated that circular polarized light emission can be obtained by controlling spin polarized charge recombination, this by utilizing the chiral layer in a light emitting diode (LED).⁶⁷ This device is named as “spin-LED”, due to the significant role of spin-polarized charge carrier caused circular polarized emission. The device synthesized and characterized in ref.⁶⁷ is based on a chiral metal-halide perovskite, where chiral centres are present in the methylbenzylammonium moiety using lead iodide. One of the advantages of using metal halide nano crystals is that they are tuneable in wavelength, with narrow spectral emission and higher quantum efficiency. These photonic related characteristics make this class of compounds promising candidates for applications in circularly polarized emission (once suitable chiral groups

are introduced within the molecular system). In this paper authors have also used the magnetic conducting probe AFM, to measure spin polarization, eventually obtaining around 80% spin polarization, a quite significant result in these systems. Featuring a 2.6% polarization degree in circularly polarized electroluminescence (CP-EL) measurements.

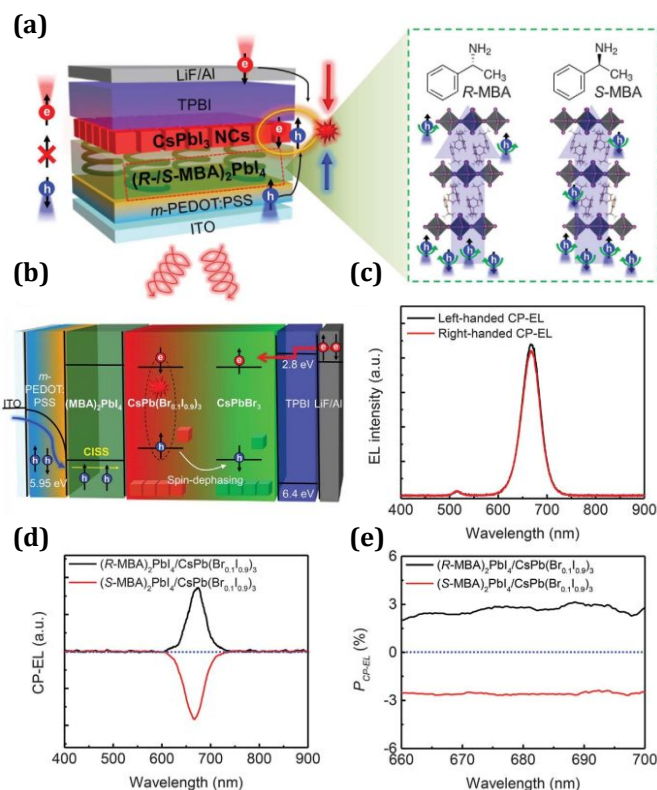


Figure 11: (a) Schematic presentation of fabricated device along with composition of the material layers demonstrating spin polarization causes by holes within the layer (b) second schematic diagram showing the spin selective charge carrier recombination and circular polarized emission. (c) showing difference in electroluminescence of left and right-handed polarization of light. (d) calculated CP-EL clearly shows the mirror symmetry in emission at ~680nm. Reproduced from reference 67 with permission from American Association for the Advancement of Science, copyright 2021.

3.2 Light induced chiral switching polymer for MR devices:

A quite interesting MR device application exploiting the CISS effect was presented in a recent article by Yamamoto⁶⁸, where a SAM of overcrowded alkene is chemisorbed on alumina. Interestingly the compound adsorbed on the substrate surface is light sensitive and works as a molecular switch, by changing its handedness upon shining light, **Figure 12**. This molecular system was utilized in the spin-valve device and was demonstrated to control magnetization by light pulses on a transparent PEDOT electrode. Authors have also assessed how switching handedness of the chemisorbed molecules plays an important role in the device performance, this in terms of controlling the spin alignment in ferromagnetic interface. Photoirradiation on junction of standard four probe geometry along with exploiting Al₂O₃ as buffer layer and bottom Ni electrode are used for this spin-valve fabrication. Antisymmetric MR response was observed from the device, the MR response switches upon shining the light along with scanning an external applied magnetic field with a ~4% change in magnetoresistance, making this system quite interesting for the application in the field of opto-electronics where circular polarized light-stimuli

are exploited. The same device showed a 44% spin polarization observed in I-V curves obtained *via* conducting magnetic AFM measurements.

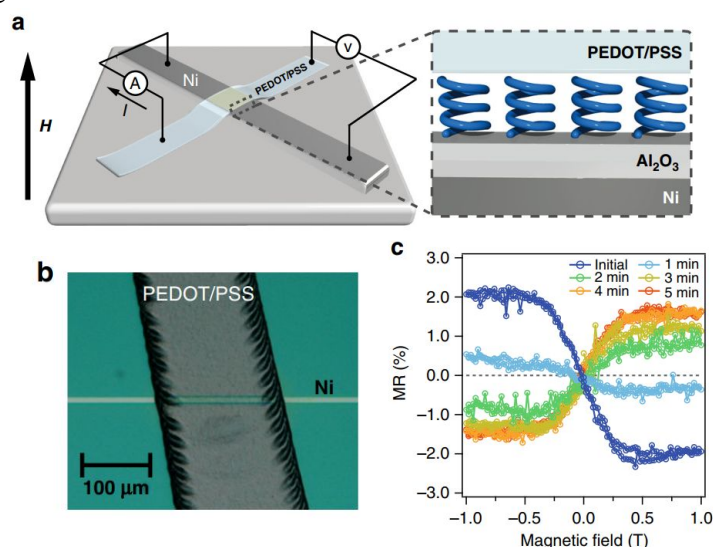


Figure 12: (a) Schematic presentation for spin valve in 4 probe geometry where top electrode is replaced by transparent conducting electrode (Inset: sandwich at cross-section) (b) SEM image of actual device (c) magnetoresistance measurement with sweeping magnetic field in between -1T to 1T at various time span. Reproduced from reference 68 with permission from Nature Publishing Group, copyright 2019.

All the above presented work demonstrates the growing field with advance way of probing the CISS effect and further utilize these materials to control the spin for spintronics application. Not only this field is limited to ether bulk or molecular level but researchers are now demonstrating this effect even in 2D materials which would help to further miniaturization existing electronics for spin-based application.

CISS effect can be utilized by using magnetized, ferromagnetic substrates which controls the enantiospecific molecule– substrate interactions and guide reaction outcomes. Figure 12(a) depict the interaction of chiral molecule with a substrate where spin is randomly aligned, because of helicity of the chiral molecule, molecular handedness is accompanied by charge polarization eventually inducing spin polarization.⁶⁹

4. Chiral-recognition, chiral-induction and CISS

A pivotal point for the design and development of innovative applications exploiting the handedness of chiral systems concerns the interplay between chirality, chiral-induction and spin-filtering. This section describes a novel perspective on the role that electron spin plays in driving intermolecular forces active between two chiral molecular systems, more in general between chiral systems (for example chiral molecules adsorbed on a surface, which eventually behaves as a surface characterized by specific handedness). The role of the spin arises from the chiral induced spin selectivity (CISS) effect, related to electrons moving in chiral systems.^{70–72} Within this field recent contributions concern the role of spin in the process of enantio-recognition. As it is demonstrated by straightforward comparison of three systems where a canonical electrochemical enantio-recognition experiment is carried out by studying the four possible combinations of a chiralized-surface with chiralized (i.e. handedness in the nanoparticle is induced via adsorption of

chiral compound) silver nanoparticles (AgNPs are used as chiralized-redox probes), exploiting the strong chemisorption of an intrinsic chiral thiophene derivative (3,3'-bibenzothiophene core functionalized with 2,2'-bithiophene wings: BT₂T₄⁷³) to impart ad-hoc handedness.

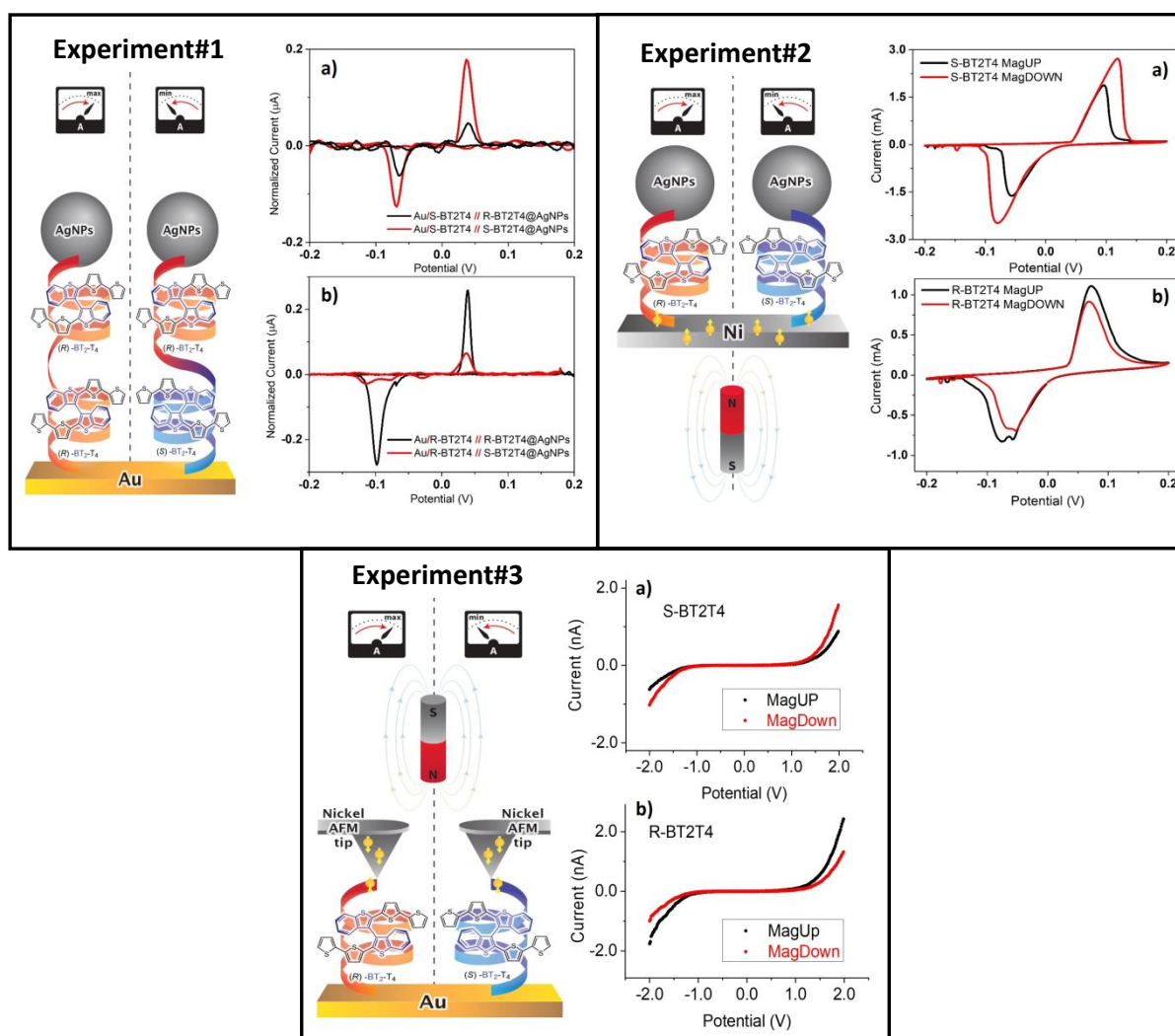


Figure 13. Experiment I: chiral recognition electrochemistry. CVs are recorded for all the possible handedness combinations: **a)** black Au|(S)-BT2T4|(R)-BT2T4@AgNP, red Au|(S)-BT2T4|(S)-BT2T4@AgNP. **b)** black Au|(R)-BT2T4|(R)-BT2T4@AgNP, red Au|(R)-BT2T4|(S)-BT2T4@AgNP. 0.1 M KCl in aqueous solution is the base electrolyte. **Experiment II:** spin-dependent CVs and its Schematic representation. **a)** Ni|(S)-BT2T4@AgNPs: black line MagUP, red curve MagDOWN. **b)** Ni|(R)-BT2T4@AgNPs: black line MagUP, red curve MagDOWN. **Experiment III:** Schematic representation of set up: magnetic conductive probe AFM. Au substrate and Ni ferromagnetic tip: black line MagUP orientation, red line MagDOWN orientation. **a)** Au|(S)-BT2T4 interface. **b)** Au|(S)-BT2T4 interface. Circle dimension in I-V curves is representative of a ± 0.1 nA sensitivity, corresponding to a 5% standard deviation on the largest current value. Right panel summarizes, by straight comparison between the electrochemical and SDE and mc-AFM data, that in the electrochemical experiment the chiralized electrode surface acts as a spin-injector. Reproduced from reference 74 with permission from Wiley-VCH Verlag, copyright 2024.

Then, close comparison with results obtained by spin-polarized interfacial charge transmission obtained in typical spin-dependent electrochemistry (cyclic voltammeteries CV) and spin-polarized

conduction (mcAFM) show that the chiralized surface behaves like a spin-polarized source/sink of electrons and moreover that the enantio-recognition process is also driven by spin/handedness interactions (the basics laying at the heart of the CISS effect). The relevant experimental results are schematically presented in Figure 13.⁷⁴

The previous results are tightly related to the induction of optical rotation in a photo-luminescence (PL) experiments, where quantum dots are adsorbed on a chiral surface.⁷⁵ Here the response of achiral core-shell CdSe/CdS quantum-dots reveals optical rotation as induced by adsorption on a chiralized layer of poly-aniline (PANI). In this case handedness is obtained by performing the electropolymerization in a solution containing an enantiopure derivative of camphor, the R- (or S-) camphor sulfonic acid.^{76,77} The relevant experimental set-up and optical rotation in PL signal is shown in Figure 14. This study is one of the kinds where CISS effect was utilized to get polarized emission at single photon level.⁷⁸

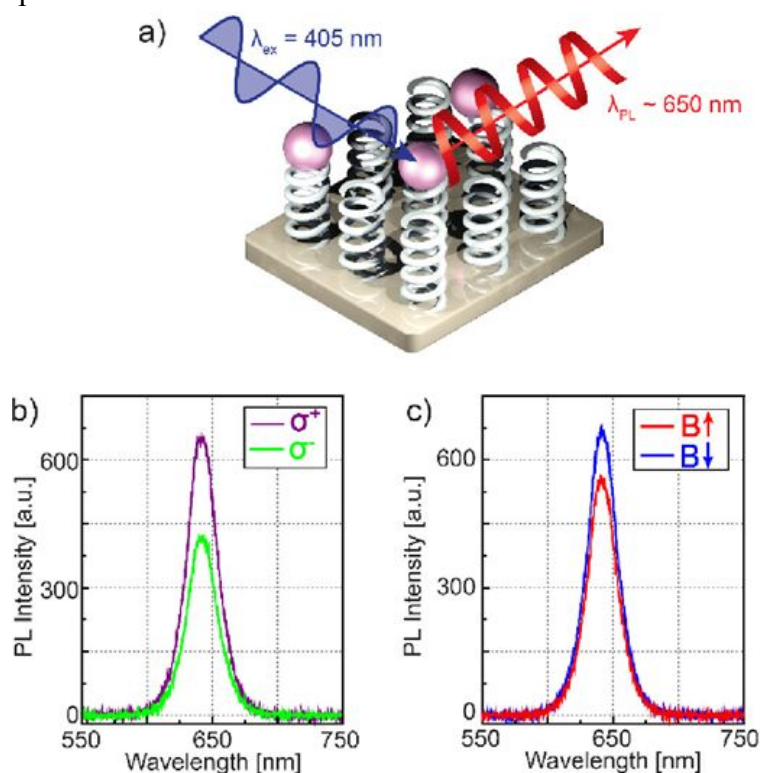


Figure 14. a) Schematic of excitation of colloidal CdSe/CdS QDs sitting on the chiral PANI surface. b) PL spectra of a 9 ML individual QD recorded for an into-plane surface magnetization showing a preferred right-handed (purple) circular polarization. c) Total photoluminescence intensity observed from the same QD for magnetization directions into (blue) and out-of (red) the surface plane. Reproduced from reference 78 with permission from American Chemical Society, copyright 2024.

Perspectives:

The latter experimental results clearly demonstrate that spin plays a significant role in driving processes where enantio-recognition (handedness) is involved. Of course, relevant applications involve both signal encoding via spectroscopic measurements as well as by electrochemically triggered processes. There is ample room to broadening and developing the active field of research in connection with the CISS effect.

- 1) 2D materials, like TMDs or perovskites, where handedness can be suitably exploited to break inversion symmetry, allowing to obtain spin-light emitting diodes (spin-LED) as recently shown by Wu and Wang chiral(amine) perovskite, characterized by an 80% spin injection polarization and a CP-EL asymmetric factor (gCP-EL) of about 1.6×10^{-2} .⁷⁹
- 2) Optical probing spin-polarization, as induced by the CISS effect by exploiting photonic materials allowing to make a quantitative measure of the polarization resolved emission induced by handedness, our group is actively exploring this research direction. See for example a recent study where 2D materials are intercalated with chiral compounds, with application in the field of spintronics.⁸⁰
- 3) Implementation of spin-controlled Q-bits based on chiral molecular architectures, as described in a recent paper based exploiting thia-bridged triarylamine hetero[4]helicene radical cation chemisorbed on gold.⁸¹

Acknowledgments

S. Mishra and A.C.J. acknowledge support from Laboratory Directed Research and Development (LDRD) Early Career Award 20220531ECR & Director's Postdoctoral fellowship 20230854PRD2. Center for Integrated Nanotechnologies (CINT). C.F. gratefully acknowledges Los Alamos National Lab Project: 2024AC0022, SONG: Spin rOle iN charGe transfer @ 2D chiralized interfaces and the Ministry of University and Research (MUR), PRIN 2022 cod. 2022NW4P2T "From metal nanoparticles to molecular complexes in electrocatalysis for green hydrogen evolution and simultaneous fine chemicals production (FUTURO)", PI Dr. Francesco Vizza

References:

- ¹ H. Sakai, and K. Yonezawa, "Remanent magnetization as a fossil of lightning current," *Proceedings of the Japan Academy, Series B* **78**(1), 1–5 (2002).
- ² J. Stöhr, and J. Siegmann, *Magnetism | SpringerLink* (n.d.).
- ³ L.D. Barron, "Magnetic molecules: Chirality and magnetism shake hands," *Nature Materials* **7**(9), 691–692 (2008).
- ⁴ L.D. Barron, "True and false chirality and absolute enantioselection," *Rend. Fis. Acc. Lincei* **24**(3), 179–189 (2013).
- ⁵ Y.P. Feng, L. Shen, M. Yang, A. Wang, M. Zeng, Q. Wu, S. Chintalapati, and C.-R. Chang, "Prospects of spintronics based on 2D materials," *Wiley Interdisciplinary Reviews: Computational Molecular Science* **7**(5), (2017).
- ⁶ H. Lu, J. Wang, C. Xiao, X. Pan, X. Chen, R. Brunecky, J.J. Berry, K. Zhu, M.C. Beard, and Z.V. Vardeny, "Spin-dependent charge transport through 2D chiral hybrid lead-iodide perovskites," *Science Advances* **5**(12), eaay0571 (2019).
- ⁷ G.L.J.A. Rikken, and E. Raupach, "Enantioselective magnetochiral photochemistry," *Nature* **405**(6789), 932–935 (2000).
- ⁸ "Snails: Right-handed or Left-handed?," *Genomics Research from Technology Networks*, (n.d.).
- ⁹ C. Diller, and C.B. Fenster, "Corolla chirality in *Hypericum irazuense* and *H. costaricense* (Hypericaceae): parallels with monomorphic enantiostyly," *The Journal of the Torrey Botanical Society* **141**(2), 109–114 (2014).
- ¹⁰ G. Laurent, D. Lacoste, and P. Gaspard, "Emergence of homochirality in large molecular systems," *PNAS* **118**(3), (2021).
- ¹¹ M. Agnes, A. Nitti, D.A.V. Griend, D. Dondi, D. Merli, and D. Pasini, "A chiroptical molecular sensor for ferrocene," *Chem. Commun.* **52**(77), 11492–11495 (2016).

- ¹² F. Sannicolò, P.R. Mussini, T. Benincori, R. Martinazzo, S. Arnaboldi, G. Appoloni, M. Panigati, E. Quartapelle Procopio, V. Marino, R. Cirilli, S. Casolo, W. Kutner, K. Noworyta, A. Pietrzyk-Le, Z. Iskierko, and K. Bartold, "Inherently Chiral Spider-Like Oligothiophenes," *Chem. Eur. J.* **22**(31), 10839–10847 (2016).
- ¹³ L. Dong, Y. Zhang, X. Duan, X. Zhu, H. Sun, and J. Xu, "Chiral PEDOT-Based Enantioselective Electrode Modification Material for Chiral Electrochemical Sensing: Mechanism and Model of Chiral Recognition," *Anal. Chem.* **89**(18), 9695–9702 (2017).
- ¹⁴ T.D. Booth, D. Wahnou, and I.W. Wainer, "Is chiral recognition a three-point process?," *Chirality* **9**(2), 96–98 (1997).
- ¹⁵ V.A. Davankov, "The nature of chiral recognition: Is it a three-point interaction?," *Chirality* **9**(2), 99–102 (1997).
- ¹⁶ D.E. Koshland, "The Key–Lock Theory and the Induced Fit Theory," *Angewandte Chemie International Edition in English* **33**(23–24), 2375–2378 (1995).
- ¹⁷ A.D. Mesecar, and D.E. Koshland, "A new model for protein stereospecificity," *Nature* **408**(6813), 668–668 (2000).
- ¹⁸ J.L. Greenfield, D. Di Nuzzo, E.W. Evans, S.P. Senanayak, S. Schott, J.T. Deacon, A. Peugeot, W.K. Myers, H. Sirringhaus, R.H. Friend, and J.R. Nitschke, "Electrically Induced Mixed Valence Increases the Conductivity of Copper Helical Metallopolymers," *Advanced Materials* **33**(24), 2100403 (2021).
- ¹⁹ F. Pop, P. Auban-Senzier, E. Canadell, G.L.J.A. Rikken, and N. Avarvari, "Electrical magnetochiral anisotropy in a bulk chiral molecular conductor," *Nat Commun* **5**(1), 3757 (2014).
- ²⁰ Y. Liang, K. Banjac, K. Martin, N. Zigon, S. Lee, N. Vanthuyne, F.A. Garcés-Pineda, J.R. Galán-Mascarós, X. Hu, N. Avarvari, and M. Lingenfelder, "Enhancement of electrocatalytic oxygen evolution by chiral molecular functionalization of hybrid 2D electrodes," *Nat Commun* **13**(1), 3356 (2022).
- ²¹ C. Wattanakit, Y.B.S. Côme, V. Lapeyre, P.A. Bopp, M. Heim, S. Yadnum, S. Nokbin, C. Warakulwit, J. Limtrakul, and A. Kuhn, "Enantioselective recognition at mesoporous chiral metal surfaces," *Nature Communications* **5**, ncomms4325 (2014).
- ²² X. Han, J. Zhang, J. Huang, X. Wu, D. Yuan, Y. Liu, and Y. Cui, "Chiral induction in covalent organic frameworks," *Nat Commun* **9**(1), 1294 (2018).
- ²³ T. van Leeuwen, W. Danowski, E. Otten, S.J. Wezenberg, and B.L. Feringa, "Asymmetric Synthesis of Second-Generation Light-Driven Molecular Motors," *J. Org. Chem.* **82**(10), 5027–5033 (2017).
- ²⁴ A. Berthod, "Chiral Recognition Mechanisms," *Anal. Chem.* **78**(7), 2093–2099 (2006).
- ²⁵ Y. Jeong, H.W. Kim, J. Ku, and J. Seo, "Breakdown of chiral recognition of amino acids in reduced dimensions," *Sci Rep* **10**(1), 16166 (2020).
- ²⁶ A. Kumar, E. Capua, K. Vankayala, C. Fontanesi, and R. Naaman, "Magnetless Device for Conducting Three-Dimensional Spin-Specific Electrochemistry," *Angew. Chem. Int. Ed.* **56**(46), 14587–14590 (2017).
- ²⁷ F. Pointillart, M. Atzori, and C. Train, "Magneto-chiral dichroism of chiral lanthanide complexes," *Inorganic Chemistry Frontiers* **11**(5), 1313–1321 (2024).
- ²⁸ K. Ray, S.P. Ananthavel, D.H. Waldeck, and R. Naaman, "Asymmetric Scattering of Polarized Electrons by Organized Organic Films of Chiral Molecules," *Science* **283**(5403), 814–816 (1999).
- ²⁹ S. Mayer, C. Nolting, and J. Kessler, "Electron scattering from chiral molecules," *J. Phys. B: At. Mol. Opt. Phys.* **29**(15), 3497–3511 (1996).
- ³⁰ J.M. Dreiling, F.W. Lewis, and T.J. Gay, "Spin-polarized electron transmission through chiral halocamphor molecules," *J. Phys. B: At. Mol. Opt. Phys.* **51**(21), 21LT01 (2018).
- ³¹ S. Mishra, A. Kumar, M. Venkatesan, L. Pigani, L. Pasquali, and C. Fontanesi, "Exchange Interactions Drive Supramolecular Chiral Induction in Polyaniline (Small Methods 10/2020)," *Small Methods* **4**(10), 2070038 (2020).
- ³² A.K. Mondal, N. Brown, S. Mishra, P. Makam, D. Wing, S. Gilead, Y. Wiesenfeld, G. Leituss, L.J.W. Shimon, R. Carmieli, D. Ehre, G. Kamieniarz, J. Fransson, O. Hod, L. Kronik, E. Gazit, and R. Naaman, "Long-Range Spin-Selective Transport in Chiral Metal–Organic

Crystals with Temperature-Activated Magnetization,” *ACS Nano* **14**(12), 16624–16633 (2020).

³³ Z. Huang, B.P. Bloom, X. Ni, Z.N. Georgieva, M. Marciessy, E. Vetter, F. Liu, D.H. Waldeck, and D. Sun, “Magneto-Optical Detection of Photoinduced Magnetism via Chirality-Induced Spin Selectivity in 2D Chiral Hybrid Organic–Inorganic Perovskites,” *ACS Nano* **14**(8), 10370–10375 (2020).

³⁴ J. Wang, B. Mao, and Z.V. Vardeny, “Chirality induced spin selectivity in chiral hybrid organic–inorganic perovskites,” *The Journal of Chemical Physics* **159**(9), 091002 (2023).

³⁵ U. Huizi-Rayo, J. Gutierrez, J.M. Seco, V. Mujica, I. Diez-Perez, J.M. Ugalde, A. Tercjak, J. Cepeda, and E. San Sebastian, “An Ideal Spin Filter: Long-Range, High-Spin Selectivity in Chiral Helicoidal 3-Dimensional Metal Organic Frameworks,” *Nano Lett.* **20**(12), 8476–8482 (2020).

³⁶ C. Kulkarni, A.K. Mondal, T.K. Das, G. Grinbom, F. Tassinari, M.F.J. Mabeoone, E.W. Meijer, and R. Naaman, “Highly Efficient and Tunable Filtering of Electrons’ Spin by Supramolecular Chirality of Nanofiber-Based Materials,” *Advanced Materials* **32**(7), 1904965 (2020).

³⁷ R. Naaman, Y. Paltiel, and D.H. Waldeck, “Chiral Molecules and the Spin Selectivity Effect,” *J. Phys. Chem. Lett.* **11**(9), 3660–3666 (2020).

³⁸ M.S. Zöllner, S. Varela, E. Medina, V. Mujica, and C. Herrmann, “Insight into the Origin of Chiral-Induced Spin Selectivity from a Symmetry Analysis of Electronic Transmission,” *J. Chem. Theory Comput.* **16**(5), 2914–2929 (2020).

³⁹ V.V. Maslyuk, R. Gutierrez, A. Dianat, V. Mujica, and G. Cuniberti, “Enhanced Magnetoresistance in Chiral Molecular Junctions,” *J. Phys. Chem. Lett.* **9**(18), 5453–5459 (2018).

⁴⁰ K. Michaeli, and R. Naaman, “Origin of Spin-Dependent Tunneling Through Chiral Molecules,” *J. Phys. Chem. C* **123**(27), 17043–17048 (2019).

⁴¹ S. Naskar, V. Mujica, and C. Herrmann, “Chiral-Induced Spin Selectivity and Non-equilibrium Spin Accumulation in Molecules and Interfaces: A First-Principles Study,” *J. Phys. Chem. Lett.* **14**(3), 694–701 (2023).

⁴² E. Medina, L.A. González-Arraga, D. Finkelstein-Shapiro, B. Berche, and V. Mujica, “Continuum model for chiral induced spin selectivity in helical molecules,” *J. Chem. Phys.* **142**(19), 194308 (2015).

⁴³ S. Dalum, and P. Hedegård, “Theory of Chiral Induced Spin Selectivity,” *Nano Lett.* **19**(8), 5253–5259 (2019).

⁴⁴ P. Hedegård, “Spin dynamics and chirality induced spin selectivity,” *The Journal of Chemical Physics* **159**(10), 104104 (2023).

⁴⁵ J. Fransson, “Vibrational origin of exchange splitting and ’ ’ chiral-induced spin selectivity,” *Phys. Rev. B* **102**(23), 235416 (2020).

⁴⁶ F. Evers, A. Aharony, N. Bar-Gill, O. Entin-Wohlman, P. Hedegård, O. Hod, P. Jelinek, G. Kamieniarz, M. Lemeshko, K. Michaeli, V. Mujica, R. Naaman, Y. Paltiel, S. Refaely-Abramson, O. Tal, J. Thijssen, M. Thoss, J.M. van Ruitenbeek, L. Venkataraman, D.H. Waldeck, B. Yan, and L. Kronik, “Theory of Chirality Induced Spin Selectivity: Progress and Challenges,” *Advanced Materials* **34**(13), 2106629 (2022).

⁴⁷ T. Liu, X. Wang, H. Wang, G. Shi, F. Gao, H. Feng, H. Deng, L. Hu, E. Lochner, P. Schlottmann, S. von Molnár, Y. Li, J. Zhao, and P. Xiong, “Linear and Nonlinear Two-Terminal Spin-Valve Effect from Chirality-Induced Spin Selectivity,” *ACS Nano* **14**(11), 15983–15991 (2020).

⁴⁸ T. Liu, and P.S. Weiss, “Spin Polarization in Transport Studies of Chirality-Induced Spin Selectivity,” *ACS Nano* **17**(20), 19502–19507 (2023).

⁴⁹ T. Liu, Y. Adhikari, H. Wang, Y. Jiang, Z. Hua, H. Liu, P. Schlottmann, H. Gao, P.S. Weiss, B. Yan, J. Zhao, and P. Xiong, “Chirality-Induced Magnet-Free Spin Generation in a Semiconductor,” *Advanced Materials* **36**(36), 2406347 (2024).

⁵⁰ Z.V. Vardeny, *Organic Spintronics* (CRC Press, 2017).

⁵¹ E. Ramsden, *Hall-Effect Sensors* (Elsevier, 2006).

- ⁵² E.Z.B. Smolinsky, A. Neubauer, A. Kumar, S. Yochelis, E. Capua, R. Carmieli, Y. Paltiel, R. Naaman, and K. Michaeli, "Electric Field-Controlled Magnetization in GaAs/AlGaAs Heterostructures–Chiral Organic Molecules Hybrids," *J. Phys. Chem. Lett.* **10**(5), 1139–1145 (2019).
- ⁵³ A. Kumar, E. Capua, M.K. Kesharwani, J.M.L. Martin, E. Sitbon, D.H. Waldeck, and R. Naaman, "Chirality-induced spin polarization places symmetry constraints on biomolecular interactions," *Proceedings of the National Academy of Sciences* **114**(10), 2474–2478 (2017).
- ⁵⁴ S. Mishra, A.K. Mondal, S. Pal, T.K. Das, E.Z.B. Smolinsky, G. Siligardi, and R. Naaman, "Length-Dependent Electron Spin Polarization in Oligopeptides and DNA," *J. Phys. Chem. C* **124**(19), 10776–10782 (2020).
- ⁵⁵ M. Kettner, B. Gohler, H. Zacharias, D. Mishra, V. Kiran, R. Naaman, C. Fontanesi, D.H. Waldeck, S. Sek, J. Pawlowski, and J. Juhaniwicz, "Spin Filtering in Electron Transport Through Chiral Oligopeptides," *J Phys Chem C* **119**(26), 14542–14547 (2015).
- ⁵⁶ F. Blumenschein, M. Tamski, C. Roussel, E.Z.B. Smolinsky, F. Tassinari, R. Naaman, and J.-P. Ansermet, "Spin-dependent charge transfer at chiral electrodes probed by magnetic resonance," *Phys. Chem. Chem. Phys.* **22**(3), 997–1002 (2020).
- ⁵⁷ R. Naaman, and D.H. Waldeck, "Spin dependent electrochemistry," in *Encyclopedia of Solid-Liquid Interfaces (First Edition)*, edited by K. Wandelt and G. Bussetti, (Elsevier, Oxford, 2024), pp. 267–277.
- ⁵⁸ R. Rodríguez, C. Naranjo, A. Kumar, P. Matozzo, T.K. Das, Q. Zhu, N. Vanthuyne, R. Gómez, R. Naaman, L. Sánchez, and J. Crassous, "Mutual Monomer Orientation To Bias the Supramolecular Polymerization of [6]Helicenes and the Resulting Circularly Polarized Light and Spin Filtering Properties," *J. Am. Chem. Soc.* **144**(17), 7709–7719 (2022).
- ⁵⁹ S. Mishra, A.K. Mondal, E.Z.B. Smolinsky, R. Naaman, K. Maeda, T. Nishimura, T. Taniguchi, T. Yoshida, K. Takayama, and E. Yashima, "Spin Filtering Along Chiral Polymers," *Angewandte Chemie International Edition* **59**(34), 14671–14676 (2020).
- ⁶⁰ S. Mishra, L. Pasquali, and C. Fontanesi, "Spin control using chiral templated nickel," *Appl. Phys. Lett.* **118**(22), 224001 (2021).
- ⁶¹ S. Ghosh, B.P. Bloom, Y. Lu, D. Lamont, and D.H. Waldeck, "Increasing the Efficiency of Water Splitting through Spin Polarization Using Cobalt Oxide Thin Film Catalysts," *J. Phys. Chem. C* **124**(41), 22610–22618 (2020).
- ⁶² P.V. Möllers, J. Wei, S. Salamon, M. Bartsch, H. Wende, D.H. Waldeck, and H. Zacharias, "Spin-Polarized Photoemission from Chiral CuO Catalyst Thin Films," *ACS Nano* **16**(8), 12145–12155 (2022).
- ⁶³ F. Calavalle, M. Suárez-Rodríguez, B. Martín-García, A. Johansson, D.C. Vaz, H. Yang, I.V. Maznichenko, S. Ostanin, A. Mateo-Alonso, A. Chuvilin, I. Mertig, M. Gobbi, F. Casanova, and L.E. Hueso, "Gate-tuneable and chirality-dependent charge-to-spin conversion in tellurium nanowires," *Nat. Mater.* **21**(5), 526–532 (2022).
- ⁶⁴ M.N. Baibich, J.M. Broto, A. Fert, F.N. Van Dau, F. Petroff, P. Etienne, G. Creuzet, A. Friederich, and J. Chazelas, "Giant Magnetoresistance of (001)Fe/(001)Cr Magnetic Superlattices," *Phys. Rev. Lett.* **61**(21), 2472–2475 (1988).
- ⁶⁵ S. Mishra, A.K. Mondal, E.Z.B. Smolinsky, R. Naaman, K. Maeda, T. Nishimura, T. Taniguchi, T. Yoshida, K. Takayama, and E. Yashima, "Spin Filtering Along Chiral Polymers," *Angewandte Chemie International Edition* **n/a**(n/a), (n.d.).
- ⁶⁶ K. Shiota, A. Inui, Y. Hosaka, R. Amano, Y. Ōnuki, M. Hedo, T. Nakama, D. Hirobe, J. Ohe, J. Kishine, H.M. Yamamoto, H. Shishido, and Y. Togawa, "Chirality-Induced Spin Polarization over Macroscopic Distances in Chiral Disilicide Crystals," *Phys. Rev. Lett.* **127**(12), 126602 (2021).
- ⁶⁷ Y.-H. Kim, Y. Zhai, H. Lu, X. Pan, C. Xiao, E.A. Gaulding, S.P. Harvey, J.J. Berry, Z.V. Vardeny, J.M. Luther, and M.C. Beard, "Chiral-induced spin selectivity enables a room-temperature spin light-emitting diode," *Science* **371**(6534), 1129–1133 (2021).
- ⁶⁸ M. Suda, Y. Thathong, V. Promarak, H. Kojima, M. Nakamura, T. Shiraogawa, M. Ehara, and H.M. Yamamoto, "Light-driven molecular switch for reconfigurable spin filters," *Nat Commun* **10**(1), 2455 (2019).

- ⁶⁹ T.S. Metzger, S. Mishra, B.P. Bloom, N. Goren, A. Neubauer, G. Shmul, J. Wei, S. Yochelis, F. Tassinari, C. Fontanesi, D.H. Waldeck, Y. Paltiel, and R. Naaman, "The Electron Spin as a Chiral Reagent," *Angewandte Chemie International Edition* **n/a**(n/a), (n.d.).
- ⁷⁰ R. Naaman, Y. Paltiel, and D.H. Waldeck, "Chirality and Spin: A Different Perspective on Enantioselective Interactions," *CHIMIA* **72**(6), 394–394 (2018).
- ⁷¹ D. Di Nuzzo, C. Kulkarni, B. Zhao, E. Smolinsky, F. Tassinari, S.C.J. Meskers, R. Naaman, E.W. Meijer, and R.H. Friend, "High Circular Polarization of Electroluminescence Achieved via Self-Assembly of a Light-Emitting Chiral Conjugated Polymer into Multidomain Cholesteric Films," *ACS Nano* **11**(12), 12713–12722 (2017).
- ⁷² D. Di Nuzzo, L. Cui, J.L. Greenfield, B. Zhao, R.H. Friend, and S.C.J. Meskers, "Circularly Polarized Photoluminescence from Chiral Perovskite Thin Films at Room Temperature," *ACS Nano* **14**(6), 7610–7616 (2020).
- ⁷³ F. Sannicolò, S. Arnaboldi, T. Benincori, V. Bonometti, R. Cirilli, L. Dunsch, W. Kutner, G. Longhi, P.R. Mussini, M. Panigati, M. Pierini, and S. Rizzo, "Potential-Driven Chirality Manifestations and Impressive Enantioselectivity by Inherently Chiral Electroactive Organic Films," *Angew. Chem. Int. Ed.* **53**(10), 2623–2627 (2014).
- ⁷⁴ A. Stefani, T. Salzillo, P.R. Mussini, T. Benincori, M. Innocenti, L. Pasquali, A.C. Jones, S. Mishra, and C. Fontanesi, "Chiral Recognition: A Spin-Driven Process in Chiral Oligothiophene. A Chiral-Induced Spin Selectivity (CISS) Effect Manifestation," *Advanced Functional Materials* **34**(2), 2308948 (2024).
- ⁷⁵ P. Roy, N. Kantor-Uriel, D. Mishra, S. Dutta, N. Friedman, M. Sheves, and R. Naaman, "Spin-Controlled Photoluminescence in Hybrid Nanoparticles Purple Membrane System," *ACS Nano* **10**(4), 4525–4531 (2016).
- ⁷⁶ E.E. Havinga, M.M. Bouman, E.W. Meijer, A. Pomp, and M.M.J. Simenon, "Large induced optical activity in the conduction band of polyaniline doped with (1S)-(+)-10-camphorsulfonic acid," *Synthetic Metals* **66**(1), 93–97 (1994).
- ⁷⁷ S. Mishra, A. Kumar, M. Venkatesan, L. Pigani, L. Pasquali, and C. Fontanesi, "Exchange Interactions Drive Supramolecular Chiral Induction in Polyaniline," *Small Methods* **4**(10), 2000617 (2020).
- ⁷⁸ S. Mishra, E.G. Bowes, S. Majumder, J.A. Hollingsworth, H. Htoon, and A.C. Jones, "Inducing Circularly Polarized Single-Photon Emission via Chiral-Induced Spin Selectivity," *ACS Nano* **18**(12), 8663–8672 (2024).
- ⁷⁹ Q. Wang, H. Zhu, Y. Tan, J. Hao, T. Ye, H. Tang, Z. Wang, J. Ma, J. Sun, T. Zhang, F. Zheng, W. Zhang, H.W. Choi, W.C.H. Choy, D. Wu, X.W. Sun, and K. Wang, "Spin Quantum Dot Light-Emitting Diodes Enabled by 2D Chiral Perovskite with Spin-Dependent Carrier Transport," *Advanced Materials* **36**(5), 2305604 (2024).
- ⁸⁰ Q. Qian, H. Ren, J. Zhou, Z. Wan, J. Zhou, X. Yan, J. Cai, P. Wang, B. Li, Z. Sofer, B. Li, X. Duan, X. Pan, Y. Huang, and X. Duan, "Chiral molecular intercalation superlattices," *Nature* **606**(7916), 902–908 (2022).
- ⁸¹ N. Giaconi, M. Lupi, T. Kumar Das, A. Kumar, L. Poggini, C. Viglianisi, L. Sorace, S. Menichetti, R. Naaman, R. Sessoli, and M. Mannini, "Spin polarized current in chiral organic radical monolayers," *Journal of Materials Chemistry C* **12**(27), 10029–10035 (2024).

Due to the nature of the present manuscript, which is a Perspective, the experimental data, as well as all the procedures, supporting this article and details concerning both calculations and data elaboration are available following the references indicated in the manuscript.